Superconductor Science and Technology

PAPER • OPEN ACCESS

Thermal contact resistance at the Nb/Cu interface as a limiting factor for sputtered thin film RF superconducting cavities

To cite this article: V Palmieri and R Vaglio 2016 *Supercond. Sci. Technol.* **29** 015004

OPEN ACCESS
IOP Publishing
Superconductor Science and Technology
Supercond. Sci. Technol. **29** (2016) 015004 (12pp)
doi:10.1088/0953-2048/29/1/015004

Thermal contact resistance at the Nb/Cu interface as a limiting factor for sputtered thin film RF superconducting cavities

V Palmieri[1] **and R Vaglio**[2]

[1] Legnaro National Laboratories—Istituto Nazionale di Fisica Nucleare (INFN), Legnaro (PD), Italy
[2] Dipartimento di Fisica, Università di Napoli Federico II, CNR SPIN e INFN—Napoli (NA), Italy

E-mail: palmieri@lnl.infn.it

Received 30 July 2015, revised 18 September 2015
Accepted for publication 7 October 2015
Published 20 November 2015

Abstract

The 'Q-slope' problem has so far strongly limited the application of niobium thin film sputtered copper cavities in high field accelerators. In the present paper, based on experimental evidence, we consider the hypothesis that the Q-slope is related to enhanced thermal boundary resistance $R_{Nb/Cu}$ at the Nb/Cu interface, due to poor thermal contact between film and substrate. We have developed a simple model that directly connects the Q versus E_{acc} curves to the distribution function $f(R_{Nb/Cu})$ of $R_{Nb/Cu}$ values at the Nb/Cu interface over the cavity surface. Starting from different Q versus E_{acc} experimental curves from different sources, using typical 'inverse problem' methods, we deduce the corresponding distribution functions generating those curves. The results show, for all the examined cases, very similar functional dependences of $f(R_{Nb/Cu})$ and prove that, to describe the experimental Q versus E_{acc} curves, it is sufficient to assume that only a small fraction of the film over the cavity surface is in poor thermal contact with the substrate. The whole body of information and data reported seems to indicate that the main origin of the Q-slope in thin film cavities is related to bad adhesion at the Nb/Cu interface. Strategies to solve the Q-slope problem improving the film adhesion are finally delineated.

Keywords: niobium copper thin film cavities, sputtering, superconducting cavities, niobium–copper interface, thermal boundary resistance, Kapitza resistance

(Some figures may appear in colour only in the online journal)

1. Introduction

From high energy physics to medical physics, as the number of uses of accelerators grows, the challenge of building high performance accelerators at low cost is becoming more and more important. In order to meet that challenge, the scientific community is exploring the application of a thin film of niobium to other materials, such as copper, in order to make less expensive and higher quality accelerator components.

High purity niobium costs around 40 times more than copper. Besides cost, another potential advantage of the niobium/copper solution concerns the higher thermal conductivity of copper with respect to that of niobium. At high radio frequency (RF) power, impurities embedded inside niobium or even defects on the surface of the superconductor can promote the formation of 'hot spots', i.e. a local heating of the superconductor. Because of the poor thermal conductivity of niobium, the heat is not as promptly transmitted to the helium bath as in the case of copper, resulting in a thermo-magnetic breakdown of the superconductor, that can suddenly quench from the superconducting to the normal state. This effect is strongly suppressed in thin film cavities.

With respect to bulk Nb cavities, thin film niobium sputtered copper cavities also display a much lower

sensitivity of the RF residual surface resistance to external dc magnetic fields. Nb/Cu cavities, for instance, do not seem to be sensitive to the magnetic earth field trapped in the superconductor during cooling by incomplete Meissner–Ochsenfield effect [1]. This property results in the possibility of skipping the magnetic shielding requirements for the cryomodules that host Nb/Cu cavities. The simple explanation of the insensitivity of Nb films to dc magnetic field penetration lies in the reduced mean free path of the Nb film with respect to the bulk, i.e. to a higher depinning frequency of the film with respect to the bulk [2].

Last but not least, a further advantage consists in a higher Q-factor at low RF power. Indeed at almost zero RF power, the cavity Q-factor is inversely proportional to the superconducting surface resistance R_s, through a geometrical constant Γ (i.e. $Q = \Gamma/R_s$) and $R_s\ (T) = R_{BCS}(T) + R_o$, where $R_{BCS}(T)$ is a contribution due to the quasi particle excitations, well described in the framework of the BCS theory, and R_o is a temperature-insensitive contribution to losses due to lattice defects, crystal dislocations, grain boundaries, trapped flux and mainly everything that is not BCS.

For thin film cavities, the low mean free path (mfp) of the niobium in film form determines a higher Q-value for Nb/Cu cavities because of a minimum in the curve of BCS losses versus the mfp corresponding to values of the residual resistivity ratio, RRR $\approx$ 30.

Niobium sputtered copper cavities were first introduced by C Benvenuti in the early 1980s at CERN for the construction of the superconducting cavities of the Large Electron Collider (LEP) [3]. Then the sputtering technology was applied in early 1990s at Legnaro National Laboratories of the INFN by one of the authors for the quarter wave resonators (QWRs) of the ALPI heavy ion accelerator [4]. The Nb/Cu technology has more recently been chosen again at CERN for the QWR fabrication at the ISOLDE ion beam facility [5].

Though the above-mentioned are three success stories, the use of Nb sputtered copper cavities in particle accelerators is not as common as desired, because thin film cavities present a severe Q decay problem with the Q quasi-exponentially decreasing as a function of the RF injected power.

In fact, in figure 1 we schematically plot the quality factor, Q of a superconducting cavity versus the accelerating electrical field E_{acc}: for bulk niobium cavities the Q-factor is almost constant versus field, whereas for niobium sputtered film cavities, the Q-value is higher at low field, but it rapidly decays versus the accelerating field.

In figure 2 real data on 1.5 GHz thin film cavities, obtained at $T = 1.7$ K at CERN, progressively optimizing the deposition conditions are reported [6]. The best cavity shows indeed a very high Q-factor, but still a significant Q-slope.

The future of superconducting particle accelerators, such as light sources, colliders, linear accelerators (LINACs), free electron lasers and energy recovery LINACs lies in the development of superconducting radio frequency (SRF) accelerating cavities. Therefore the Q-slope affecting thin film cavities prevents their use in any accelerator, among the above-mentioned, where high fields are required.

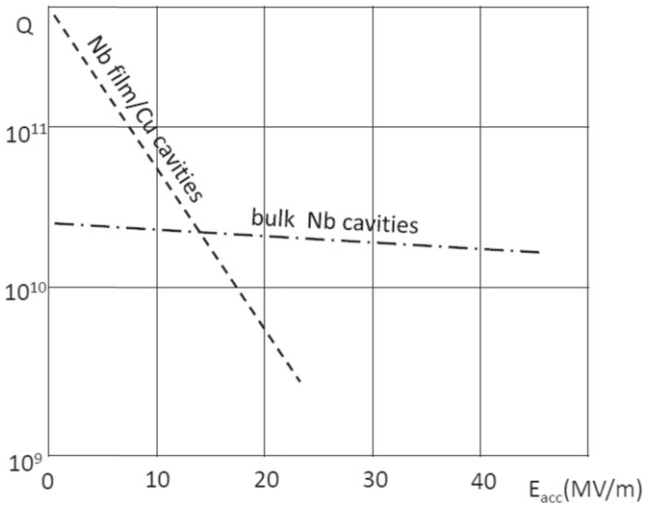

Figure 1. Q-factor versus the accelerating field for bulk niobium cavities compared to Nb film sputtered cavities. Typical behavior is schematically reported for 1.3–1.5 GHz cavities at low temperatures (1.7–1.8 K).

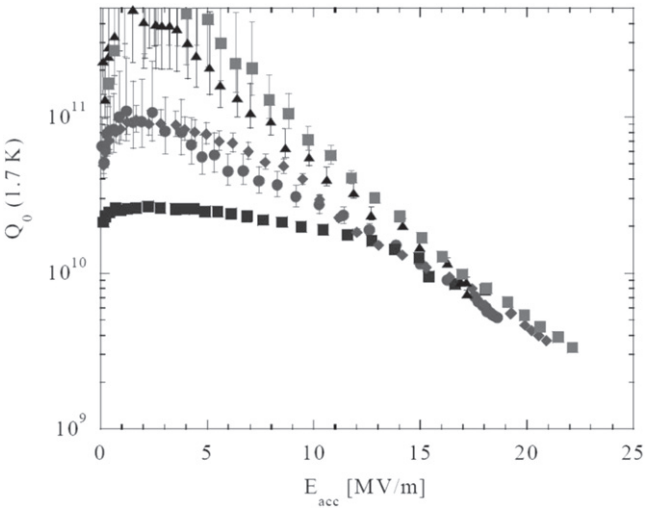

Figure 2. CERN results for 1.5 GHz cavities, from [6]. Different symbols refer to cavities of different quality.

As will be discussed in the following section, many mechanisms and related models were considered to explain this strong 'Q-slope' effect, however not one has been considered fully satisfactory in the literature, contradicting at least in part the experimental evidence.

The scope of the present paper is to introduce a new, effective model based on the presence of local high thermal resistances between the Nb sputtered film and the Cu bulk cavity, due to Nb/Cu adhesion problems, or other mechanisms generating an imperfect thermal contact at the interface.

2. Mechanisms considered for the *Q*-slope effect and experimental attempts to overcome the problem

The reason underlying the strong decay of the Q-factor versus the accelerating field in thin film cavities is still unknown and,

as mentioned in the introduction, understanding the reasons behind the Q-drop would be the first step in solving the problem and in this way accessing high performance thin film cavities at low cost. A Q decay effect is also present, to a lesser extent, in bulk niobium cavities and many researchers have proposed several models in order to explain the Q-slope (or Q-drop) mechanism [7, 8], mostly trying to justify the difference between the film and bulk cavities on the basis of the lower film residual resistivity ratio (RRR).

Attanasio *et al* [9], following the model proposed by Hylton *et al* on high critical temperature superconductors (HTCSs) [10], consider a superconducting polycrystalline niobium film as a network of Josephson junctions, leading to a field amplitude dependence of the surface resistance.

Bonin and Safa also explained the RF field limitations and residual surface resistance of superconductors in terms of their polycrystalline nature: energy dissipation arises in their model when the superconducting current exceeds the critical current of the weak-link between grains [11].

Benvenuti *et al* attribute the field-dependent resistive losses to the presence of trapped magnetic flux in niobium superconducting films. Noble gas atoms trapped in the film during film growth act as pinning centers, while the depinning increases with the increase of the accelerating field inside the resonator [12–14].

Kulik and Palmieri instead hypothesized that a possible cause for the Q-drop was the dependence of the superconducting energy gap Δ on the superfluid velocity. The gap will indeed 'close' more and more the higher the supercurrent is, i.e. the higher the accelerating field is, and the rapidity of the gap decrease depends on the niobium purity as measured by the RRR [15].

Based on these ideas the experimental efforts were mostly directed towards an improvement of the Nb film superconducting properties and increasing the RRR.

An extensive work was performed for instance at CERN [16], preparing high RRR niobium sputtered cavities by using Ne, Ar, Kr, Xe and their mixtures as sputtering gases. The result was that the best cavity performances were obtained by sputtering with krypton gas instead than the standard argon as process gas, however the overall cavity performance improvement was not relevant.

It is known that in elliptical cavities the Q-slope is higher the more the cavity shape is oblate [17] and that the superconducting properties of Nb, as well as the RRR, directly depend on the angle between the niobium target and the copper substrate [18]. So, attempts were made to sputter niobium from a cathode shape that follows the cavity geometry [19, 20]. However, though the sputtered samples indeed showed better superconductivity and overall quality parameters, the Q-factor versus field did not benefit much from having deposited from the cavity-shaped target.

Likewise, the introduction of a bias in the magnetron-sputtering configuration, and the consequent densification of the niobium films [21], did not give any significant benefit to the solution of the Q-drop problem.

We should also mention the cylindrical magnetron cavity coating configuration adopted at CERN and then at INFN, where the target is a hollow cylinder of the same length of the cavity and an internal coil is moved inside [16]. In this way the whole cavity surface is coated by a plasma ring that efficiently spans the whole target. However, even this change of the shape of the magnetron target did not improve the situation. Similarly, at Saclay Laboratories, cavities were coated by means of a movable short niobium cathode containing a permanent magnet in its interior [22]. However, the as-sputtered cavities still displayed the usual, relevant Q-slope.

Again, Nb/Cu cavities produced by a totally different sputtering technique, high-power impulse magnetron sputtering (HIPIMS), showed a very high Q-factor at high fields, but again unsatisfactory results for the Q-slope [23].

Since all attempts to improve the film deposition techniques did not give the expected results, some authors considered the possible hydrogen or oxygen diffusion in the film from the copper substrate.

Hydrogen is a well known source of contamination [24], and one could suppose that hydrogen is permeating across copper and diffusing inside niobium while growing the film. However, several attempts made at CERN to block hydrogen depositing a titanium under-layer between copper and niobium in order to getter hydrogen, gave no result on the Q-slope. The niobium films behaved in all respects like standard films coated on simple copper [25].

Oxygen could also diffuse from copper into the film. However, there is experimental evidence that for Nb film cavities, an oxidized copper surface works even better than a pure copper surface [26]. The Q-drop was consistently larger for Nb films grown on fully oxide-free copper substrate than for standard ones, proving that the oxide layer is even beneficial rather than poisonous.

Finally, it is important to also discuss here the Q-slope effect related to the so-called 'thermal feedback model' [27]. In a few words, the power dissipated by the RF field to sustain the accelerating field, $P_d = \frac{1}{2}R_s(T)H_{RF}^2$ (H_{RF} is the peak amplitude of the surface magnetic field) produces a temperature difference ΔT between the inner superconducting cavity surface and the helium bath, proportional to P_d and to the overall thermal boundary resistance R_B. This induces a thermal feedback, since, fixing the H_{RF} value, the power leads to a temperature increase followed by a surface resistance increase and by a further power increase. The overall effect is a moderate Q-slope at low fields rapidly increasing approaching the thermal runaway field, where the dissipated power diverges and the cavity undergoes a global quench. The magnitude of the Q-slope in this model depends on the thermal boundary resistance R_B between the inner cavity surface and the bath, that in turn depends on the cavity material thermal conductance and the Kapitza thermal resistance between the cavity external wall and the He bath. As will be discussed in more detail in sections 4, 5, the Nb/Cu interface thermal resistance should be, in principle, negligible. The Kapitza resistance is essentially equivalent for the Nb/He and the Cu/He interfaces, so that the higher Cu thermal conductivity with respect to niobium should play in favor of

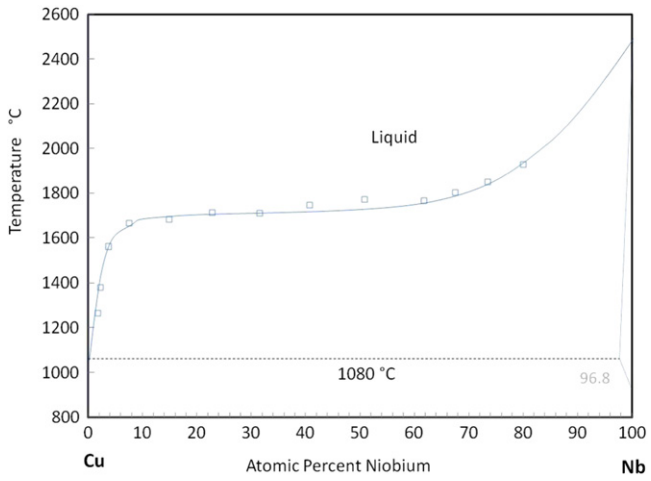

Figure 3. The Cu/Nb phase diagram, from D J Chakrabarti and D E Laughlin [28].

the thin film cavities, where thermal feedback effects should be less relevant with respect to bulk cavities.

In summary, though the whole mechanism described in this section to justify the Q-slope is possibly at work in real cavities, there has been no strong experimental evidence that really convinced the superconducting accelerating cavity community in favor of a specific one as the main actor. At the same time, all experimental attempts to reduce the Q-slope in thin film cavities by improving the film quality essentially failed.

3. The Nb/Cu interface

In the previous section, we have shown that, independently of the Nb film quality, the Q-slope problem is always present. This would suggest that the problem lies somewhere else.

Indeed, a sputtered Nb/Cu thin film cavity can be described as a set of three subsystems: (i) the superconducting niobium film; (ii) the copper substrate; (iii) the niobium–copper interface.

Excluding the first two, we will concentrate here on the Nb/Cu interface.

The first consideration is that, at the usual film deposition temperature (150 °C), there is no miscibility range between copper and niobium in the equilibrium phase diagram (see figure 3) [28].

The Nb/Cu system is indeed considered a classical example for non-miscible systems.

The problem of Nb film adhesion on a Cu substrate has been poorly investigated and is not well understood. In some cases the Nb film can peel off immediately after the sputtering and the fault is generally attributed to a non-perfect chemistry treatment of the copper substrate. In some other cases, from the author's experience, the Nb film can partially peel off even after many years, due to stress release inside the film. Other evidence has been given of film peeling found in some 352 MHZ 4-cell elliptical cavities when dismounted from the LEP at CERN [29], several years after their operation.

Moreover, the only niobium coated copper cavity deposited by cathodic arc plasma by an Italo-Polish collaboration was not measured for the same reason [30], and a thin film cavity realized by filtered cathodic arc by the Alameda Corporation gave a rather low Q-value and maximum accelerating field of 9 MV m^{-1}, and was attributed to Nb film peeling [31].

Further evidence for the relevance of film adhesion problems are listed below:

- Niobium sputtered QWRs almost never peel off. Indeed while standard magnetron sputtered cavities were sputtered at CERN at a maximum temperature of 150 °C, the QWRs were sputtered at a temperature ranging from 500–700 °C. The adhesion is improved both by the higher potential of the bias-diode technique, and by the higher temperature.
- As already mentioned, the Nb film sputtered onto onsite pre-sputtered oxide-free copper performed systematically worse with respect to films sputtered onto an oxidized copper surface. This is consistent with the hypothesis of a monotectic reaction occurring in the Cu/Nb system induced by oxygen impurities [33].

On the other side, cavities realized by an explosively bonded Nb/Cu bilayer gave excellent results (Q factors over 10^{10} and maximum accelerating fields close to 40 MV m^{-1}) [32], possibly due to the better film adhesion in this latter case, related to higher deposition energy leading to full penetration bonding.

Finally it is clear that any defect on the Cu substrate is strongly amplified by the film growth and that the adhesion between Nb and Cu, even in the absence of surface defects, is certainly influenced by lattice parameter matching at the crystalline level, so that the adhesion of Nb grown on a Cu $\langle 100 \rangle$ plane will be different from that of Nb growing on a $\langle 110 \rangle$ or $\langle 111 \rangle$ plane. We consider therefore that the problem of poor thermal contact of the film to the substrate could be far more important that commonly believed. A comprehensive review of Nb growth on Cu has been given by Valente-Feliciano [34].

4. Thermal model for the Nb/Cu interface in the presence of adhesion problems

In our opinion, all the indications presented above give strong support to the idea that in most cases the Nb film is not strongly bonded over the full cavity surface at the interface with the Cu substrate, being indeed only loosely coupled in some portion of the surface itself.

The reason for poor thermal contact at the Nb/Cu interface can be many-fold, but mainly determined by the following factors:

– Bad adhesion between niobium and copper: pure niobium and pure copper cannot have any interaction and unless they are not intermixed, they will never adhere.

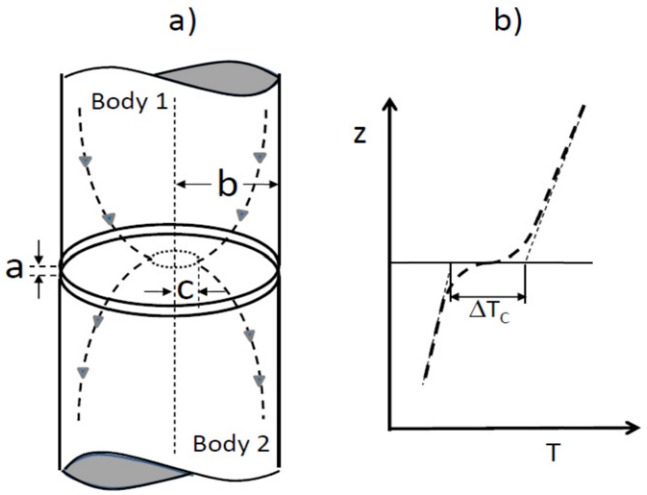

Figure 4. (a) Schematic representation of the elemental flow channel. (b) Expected temperature profile (redrawn from [37]).

- Stress inside the film: niobium films made by sputtering will always be stressed. With time, stress will relax and detach the film, inducing poor thermal contact between the two surfaces.
- Copper oxides, powder or other surface contamination: here, even if the film is adherent to the substrate, a poor thermal link exists between the niobium film and the copper substrate.
- Micro-voids at the interface: due to the effect of self-shadowing of the film growth, some micro-areas at the nucleation level can be masked by the growing film. Substrate roughness enhances this phenomenon.

In the presence of these physical situations, modeling the heat flow between the Nb film and the Cu substrate is far from being trivial. Just to give an example, in the following we will briefly review a simple model developed in the 1960s [35–38] to describe the situation of two solid sheet surfaces set in contact under vacuum with heat flowing normally from one body to the other.

The model assumes that the two solid surfaces touch only in a limited number of spots (n contact points per unit area) and analyzes the single contact point to determine its specific heat conductance using the classical heat flow equations with appropriate boundary conditions.

In [37] the single contact spot (elemental flow channel) is modeled as described in figure 4(a): two cylindrical bodies are separated by a short distance a. The radius of the cylinders is b and they touch on a restricted flat circular surface area of radius c ($c < b$).

The resulting temperature distribution is quite complicated and three-dimensional. The temperature profile along the z-axis is sketched in figure 4(b) (the temperature profile is assumed to be continuous along the interface). The contact thermal boundary conductance h_c is defined through the relation:

$$\dot{Q} = h_c \Delta T_c \tag{1}$$

where $\dot{Q}$ is the heat flow per unit area and ΔT_c is defined as shown in figure 4(b). The calculation assumes a constant temperature along the two cylinders' separation plane ($z = 0$) and a large contact area radius with respect to the cylinders' separation a ($a \ll c$).

The resulting expression for the single contact conductance is :

$$h_c = 2k\frac{c}{\pi b^2} \cdot \frac{1}{\psi} \tag{2}$$

With $k = \frac{2k_1k_2}{k_1+k_2}$ (k_1 and k_2 are the two bodies' thermal conductance) and ψ is a quasi-linear decreasing function of the ratio c/b, being 1 for $c/b = 0$ and extrapolating to 0 for $c/b \sim 0.75$.

Of course the individual contacts' shape, dimensions and distribution depend on the local surface characteristics (roughness, waviness etc) and can vary along the surface area.

For a regular array of multiple contacts equation (2) becomes:

$$h_c = 2k\frac{nc_m}{\psi} \tag{3}$$

where n is the average number of elemental flow channels per unit area and c_m is the average radius of the contact area.

In [35–38] the interface Kapitza thermal conductance h_k between the two bodies is not considered. This is fully justified at room temperature where, due to the large number of phonons, the very limited phonon acoustic mismatch and the electron contribution, the thermal boundary conductance is very high. The value can be easily estimated within the existing theoretical models [39] and is of the order of $10^6\,\mathrm{W\,cm^{-2}\,K}$, as confirmed by a number of experimental measurements [40, 41]. If the contact occurs only over an effective area A_{eff} as assumed in the model, the Kapitza effective contribution would be:

$$h_k^{\mathrm{eff}} = h_k\frac{A_{\mathrm{eff}}}{A} = h_k n\pi c_m^2 \tag{4}$$

where n and c_m have the same meaning as above. This would give in any case large conductance values at room temperature. However at low temperatures the Kapitza contribution changes dramatically, since the phonon contribution to conductivity decreases as T^3 and the electron contribution can be neglected for Nb in the superconducting state.

More generally, within this model, considering both contributions at low temperatures, the overall system thermal boundary resistance $R_{1/2}$ would be given by :

$$R_{1/2} = h_{1/2}^{-1} = (h_c)^{-1} + \left(h_k^{\mathrm{eff}}\right)^{-1} = \frac{\psi}{2knc_m} + \frac{1}{h_k n\pi c_m^2} \tag{5}$$

To give a numerical example, let us assume $n = 10^9\,\mathrm{cm^{-2}}$, $c_m = 10\,\mathrm{nm}$ (these values could be reasonable in the hypothesis of micro-voids due to roughness) $k_1 = 2\,\mathrm{W\,cmK^{-1}}$ appropriate for Cu, [42]), $k_2 = 0.1\,\mathrm{W\,cmK^{-1}}$, (appropriate for Nb [43]) and $h_k \approx 3\,\mathrm{W\,cm^{-2}\,K}$ (assuming the 'radiation limit' value, due to the substantial absence of phonon

mismatch between Nb and Cu [39]). With these input data equation (5) gives $R_{1/2} \approx 100\,\mathrm{cm^2\,K\,W^{-1}}$. Different values of the input parameters and a different choice of n and c_m would lead, of course to different $R_{1/2}$ values.

As shown in the proposed example, due to roughness, equation (5) can lead to a high thermal resistance value between two surfaces in contact under vacuum. Though the model discussed above was developed for two metal surfaces in contact, a physical situation that is somewhat different from that of a film deposited on a substrate, it nevertheless gives clear indications that a loose interface physical contact of different origins can lead to high values of the thermal contact resistance, strongly varying along the contact surface area.

We will discuss, in the forthcoming sections, the possibility that the occurrence of high values of the thermal boundary resistance between Nb and Cu $R_{\mathrm{Nb/Cu}}$ in some spots of the cavity surface, due to the weak contact of the Nb film to the Cu substrate, is the main factor determining the high Q-slope observed in Nb thin film coated Cu cavities.

5. Effect of the Nb/Cu interface on the quality factor in the presence of adhesion problems

In section 2, we discussed the thermal feedback model as a possible origin of Q-slope problems. The effect is indeed proportional to the overall thermal resistance R_{B} between the inner superconducting cavity surface and the helium bath. In Nb bulk cavities (sheet thickness d) the thermal resistance is due to the Nb conductance (k) and the Nb/HeII Kapitza resistance, i.e. $R_{\mathrm{B}} = d/k + R_{\mathrm{K}}$. The Kapitza resistance R_{K} strongly depends on the cavity external surface morphology, ranging approximately in the interval $1\text{–}10\,\mathrm{cm^2\,K\,W^{-1}}$ at 1.8 K, dominating the system thermal resistance for high RRR cavities [42, 44].

Thermal effects in bulk Nb cavities have been extensively discussed in the past [45, 46]. In a recent paper [47], the role of the thermal boundary resistance at the Nb–He interface on the superconducting accelerating cavity performances has been reconsidered, and it was demonstrated that it can play an important role in determining the cavity Q-slope problem and the maximum accelerating field, especially for high frequency cavities.

For thin film Nb/Cu cavities the overall thermal boundary resistance should be $R_{\mathrm{B}} = d_1/k_1 + d_2/k_2 + R_{\mathrm{K}} + R_{\mathrm{Nb/Cu}}$ (1: Cu, 2: Nb). The first two terms are certainly negligible: the first for the high Cu thermal conductance, the second for the small film thickness. The Kapitza resistance to be considered here is that at the Cu/HeII interface. The literature data at 1.8 K give $R_{\mathrm{K}} = 2\text{–}4\,\mathrm{cm^2\,K\,W^{-1}}$ [48–50], i.e. in the same range as the Nb/HeII Kapitza resistance values. As discussed in the previous section, if adhesion problems at the Nb/Cu interface are not considered, the thermal contact resistance should be:

$$R_{\mathrm{Nb/Cu}} = 1/h_k \approx 0.3\,\mathrm{cm^2\,K\,W^{-1}}$$

and would be negligible with respect to the Cu/He Kapitza resistance.

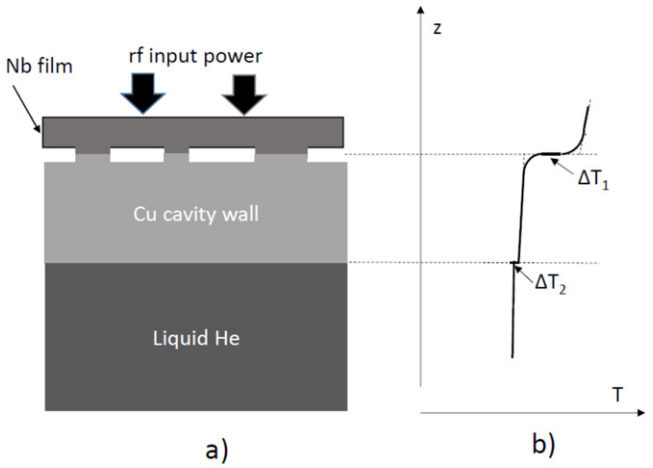

Figure 5. Schematic view of the adopted one-dimensional thermal model (a) and the related temperature profile (b).

Indeed, within this hypothesis, the possible role of thermal effects in Nb sputtered cavities was deeply analyzed at CERN, as discussed in [51], but the conclusion was negative. The authors also tried to directly measure the temperature difference ΔT between the inner Nb cavity surface and the helium bath by adsorbing helium gas (less than one monolayer) on the film surface and measuring its equilibrium pressure during RF operation, but no detectable temperature increase was observed.

However if we consider that the Nb film is indeed weakly bonded to the Cu substrate at least in limited cavity surface portions (as discussed in sections 3, 4) then the Nb/Cu boundary resistance can become high in those areas and fully dominate the heat conduction there.

In this hypothesis, locally, the temperature distribution along the direction normal to the cavity surface (in a 'one-dimensional' approximation) is reported in figure 5.

As an example, considering the contact parameters already used in section 4 for partially detached films, we would have, at low temperature (1.8 K), in the given example: $R_{\mathrm{Nb/Cu}} = 110\,\mathrm{cm^2\,K\,W^{-1}}$.

This value for the Nb/Cu interface thermal resistance is far above the typical values for the Cu/HeII Kapitza resistance at the same temperature. Therefore we would have $\Delta T = \Delta T_1 + \Delta T_2$, with $\Delta T_1 \gg \Delta T_2$ (of course we can in any case neglect here the effect of the thermal resistance of bulk Cu and Nb film).

The local value of $R_{\mathrm{Nb/Cu}}$ will not be constant over the cavity surface: indeed, in the simple model presented in the previous paragraph, it will depend on the number (n) and dimension (c_m) of the effective thermal contact spots in the partially detached film regions, that will have some statistical distribution over the cavity surface.

We can therefore introduce a statistical distribution function $f(R_{\mathrm{Nb/Cu}})$ of the $R_{\mathrm{Nb/Cu}}$ values over the whole cavity surface, that will satisfy the following conditions:

$$\int_0^\infty f\left(R_{\mathrm{Nb/Cu}}\right)\mathrm{d}R_{\mathrm{Nb/Cu}} = 1 \qquad (6)$$

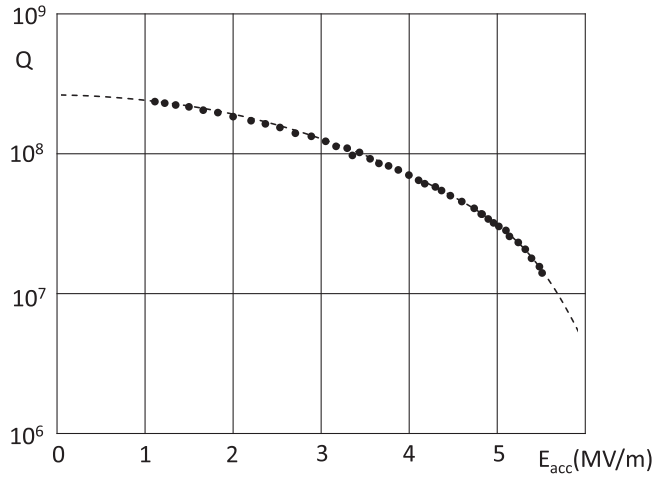

Figure 6. Q-factor versus accelerating field for a thin film Nb/Cu 6 GHz cavity at $T = 1.8$ K. The dots are the experimental points, the dashed line represents the data fitting using the distribution function $f(R_{\mathrm{Nb/Cu}})$ reported in figure 7.

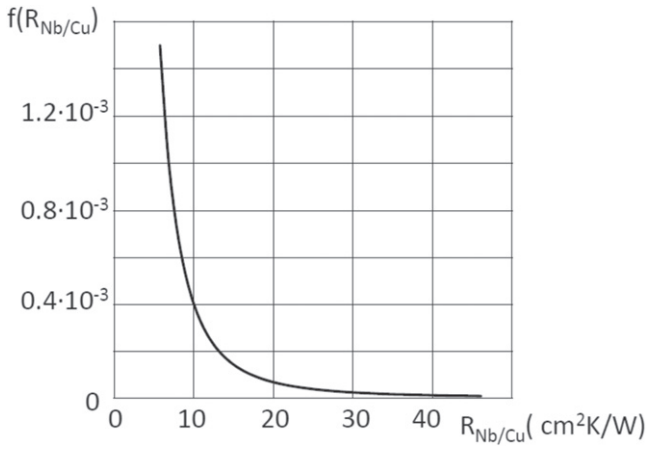

Figure 7. Distribution function $f(R_{\mathrm{Nb/Cu}})$ obtained by inverting equation (11) using as input data the Q-E_{acc} data reported in figure 6.

$$\int_0^{\infty} R_{\mathrm{Nb/Cu}} f\left(R_{\mathrm{Nb/Cu}}\right) \mathrm{d}R_{\mathrm{Nb/Cu}} = \overline{R_{\mathrm{Nb/Cu}}} \tag{7}$$

where $\overline{R_{\mathrm{Nb/Cu}}}$ is the average value of the Nb/Cu thermal boundary resistance over the cavity surface.

In the presence of non-constant values of the surface resistance over the cavity surface (keeping the assumption of a constant RF field value), the quality factor of an accelerating cavity can be expressed as:

$$Q = \frac{\Gamma}{\overline{R_{\mathrm{s}}}} \tag{8}$$

where Γ is a constant related to the cavity geometry (temperature and field independent), with $\Gamma = 290\,\Omega$ for beta 1 electron cavities, and $\overline{R_{\mathrm{s}}}$ is the average surface resistance.

Now we can calculate the Q-slope within the 'thermal feedback model' in the presence of a distribution of the contact thermal resistance at the Nb/Cu interface due to bad adhesion problems. We will use for the superconductor surface resistance the dirty-local limit explicit expression, that, at temperatures $T < 1/2T_{\mathrm{c}}$ is given by:

$$R_{\mathrm{S}}(T) = \frac{A\omega^2}{T_0 + \Delta T} \exp\left[-\frac{\Delta_0}{K_{\mathrm{B}}\left(T_0 + \Delta T\right)}\right] + R_{\mathrm{o}} \tag{9}$$

with T_{o} being the helium bath temperature, Δ_0 the low temperature value of the energy gap, K_{B} the Boltzmann constant and A a weakly frequency dependent constant, whose value is determined by the material parameters. ΔT is the temperature difference between the inner cavity wall and the helium bath, due to the finite overall thermal conductance of the cavity (including material conductivity and thermal boundary conductance at media separation). For relatively small values of ΔT it is $\Delta T = R_{\mathrm{B}} P_{\mathrm{d}}$ where R_{B} is the overall thermal resistance (from the inner cavity surface to the He bath) and P_{d} is the RF power dissipated per unit area at the inner cavity surface, given by $P_{\mathrm{d}} = \frac{1}{2} R_{\mathrm{s}}(T_{\mathrm{o}}) H_{\mathrm{RF}}^2$. Therefore:

$$\Delta T = R_{\mathrm{B}} \frac{1}{2} R_{\mathrm{s}}(T) \left(\frac{k}{\mu_o}\right)^2 E_{\mathrm{acc}}^2 \tag{10}$$

(H_{RF} is proportional to the accelerating field E_{acc} through the relation: $H_{\mathrm{RF}} = \left(k/\mu_{\mathrm{o}}\right) E_{\mathrm{acc}}$, with $k = 4.5$ mT (MV m^{-1}) [52]).

Combining equations 9 and 10 we get a dependence of the surface resistance on the accelerating field, that will depend in turn on the thermal boundary resistance being more and more relevant for increasing R_{B} values. As already discussed, increasing the RF field determines an increase in ΔT that produces an increase in $R_{\mathrm{s}}(T)$, that produces a further increase in ΔT. The process continues up to an equilibrium point, or, over a certain RF field value (quench field), can diverge, determining a 'thermal runaway' effect. Over the quench field the superconducting surface will become normal, and the surface resistance will have its normal state value R_{sn} (at GHz frequencies the RF field penetration in the Nb film will be smaller than the film thickness).

The solution of the two coupled non-linear equations 9 and 10 can be found by iteration. For any assigned value of E_{acc} one calculates ΔT from equation 10, inserting for $R_{\mathrm{s}}(T)$ the $\Delta T = 0$ value calculated from equation 9. The ΔT value calculated from 10 is then inserted in 9 to compute a new value of $R_{\mathrm{s}}(T)$ that is in turn reinserted in equation 10 to compute a further value of ΔT. The process is iterated up to convergence (or divergence over the quench field). Within this calculation scheme in some sense the iteration cycles play the role of time in the real experiment.

By this method the expected surface resistance dependence on the accelerating field E_{acc}, for each value of overall thermal resistance R_{B}, i.e. $R_{\mathrm{s}} = R_{\mathrm{s}}(T_{\mathrm{o}}, E_{\mathrm{acc}}, R_{\mathrm{B}})$ can be easily calculated. Above the quench field we assume $R_{\mathrm{s}} = R_{\mathrm{sn}}$, where R_{sn} is the normal state value of the surface resistance.

For Nb/Cu cavities we can write $R_{\mathrm{B}} = R_{\mathrm{K}} + R_{\mathrm{Nb/Cu}}$ with R_{K} being the value of the Cu/He Kapitza resistance at the temperature T_{o} and $R_{\mathrm{Nb/Cu}}$ the value of the Nb/Cu contact

Table 1. Input parameters used to invert the data for the 6 GHz cavity reported in figure 6.

T_o	$A\omega^2$	Δ_o/K_B	R_0	R_{sn}	R_K
1.8 K	$6^*10^{-3}\,\Omega\,K^{-1}$	17.5 K	0.8 $\mu\Omega$	0.01 Ω	3 $cm^2\,K\,W^{-1}$

Table 2. Input parameters used to invert the data for the 6 GHz cavity reported in figure 8.

T_o	$A\omega^2$	Δ_o/K_B	R_0	R_{sn}	R_K
1.7 K	$5^*10^{-5}\,\Omega\,K^{-1}$	18.4 K	0.6 nΩ	0.005 Ω	3 $cm^2\,K\,W^{-1}$

resistance. Since $R_{Nb/Cu}$ changes over the cavity surface as described by the statistical distribution function $f(R_{Nb/Cu})$, the average value of R_s that will determine the Q-value will be given by the integral equation:

$$\overline{R_s(T_o, E_{acc})} = \int_0^\infty R_s(T_o, E_{acc}, R_B) f(R_{Nb/Cu}) dR_{Nb/Cu}$$
$$Q = \frac{\Gamma}{\overline{R_s(T_o, E_{acc})}}. \quad (11)$$

This indicates that the $Q(E_{acc})$ curve in Nb/Cu cavities will critically depend on the $R_{Nb/Cu}$ distribution function $f(R_{Nb/Cu})$ that would depend, in the model discussed in section 4, on the distribution over the cavity surface of the density (n) and dimensions (c_m) of the effective thermal contact spots in the partially detached regions.

Unfortunately there is no way to independently estimate or measure the function $f(R_{Nb/Cu})$ with non-destructive methods, and even destructive methods would not be sufficiently accurate.

However, given the experimental $Q(E_{acc})$ curve we can calculate $\overline{R_s(T_o, E_{acc}, R_B)}$ and then invert equation 11 (which belongs to the class of first type Fredholm integral equations) and infer the statistical distribution function $f(R_{Nb/Cu})$. This is indeed a classical 'inverse problem', to obtain a numerical solution, the integral 11 has been approximated by appropriate discretization (quadrature) procedures reducing the problem to a well conditioned linear algebraic problem [53]. The data have been sampled at 15 discrete points. In this way the function f is obtained by points and its approximate analytical expression can then be reconstructed by interpolation.

In figure 6 we report the Q versus E_{acc} experimental data points for one of our Nb-coated Cu 6 GHz cavities measured at $T = 1.8$ K. The cavity is seamless and was realized by spinning from a copper circular blank. The measurement apparatus and techniques are the same described in [47]. The theoretical fit (dashed curve) has been obtained by equation (11) , computing the function $R_s(T_o, E_{acc}, R_B)$ by iteration as discussed above (equations 9, 10) up to E_{acc} values that lead to convergence and setting $R_s = R_{sn}$ above that value. The parameters used for the R_s computation are reported in table 1, and have been determined by fitting the experimental low power R_s temperature dependence.

The R_K value for the Cu/HeII interface has been set at the center of the literature value range [48–50]. This value would lead to a global thermal quench of the cavity over 12 MV m^{-1}, well outside the measurement range.

The continuous curve reported in figure 7 interpolates the data points obtained for $f(R_{Nb/Cu})$ solving the inverse problem, and corresponds to a slightly modified power law expression: $f(R_{Nb/Cu}) = 7.82 R_{Nb/Cu}^{-(4.44-0.205 \ln R_{Nb/Cu})}$. The detailed dependence of $f(R_{Nb/Cu})$ depends slightly on the specific parameters choice (table 1) and by the chosen discretization procedure, but its general characteristics are fully stable.

The function $f(R_{Nb/Cu})$ could only be evaluated for $R_{Nb/Cu} > 6\ cm^2\,K\,W^{-1}$, since lower $R_{Nb/Cu}$ values would give a significant effect only for fields outside the measurement range (over 6 MV m^{-1}).

The surprising result here is that the integral I under the represented curve is:

$$I = \int_6^\infty f(R_{Nb/Cu}) dR_{Nb/Cu} = 0.005.$$

This means that only 0.5% of the Nb film in poor thermal contact with the Cu substrate determines the observed Q versus E_{acc} curve. For $R_{Nb/Cu} < 6\ cm^2\,K\,W^{-1}$, in principle we can assume that all the remaining weight of the $f(R_{Nb/Cu})$ function (99.5%) is given by a delta function corresponding to $R_{Nb/Cu} = 0$ (perfect adherence on 99.5% of the cavity surface). Of course any other assumption respecting the condition imposed by equation (6) would lead to the same data fitting.

The strong Q-slope at low fields, within this model, is linked to the high $R_{Nb/Cu}$ values 'tail' of the statistical distribution function. High values of $R_{Nb/Cu}$ imply locally high thermal resistance (R_B) values and therefore low local quench fields. By increasing the field the Nb film areas in loose contact with the Cu substrate will be gradually driven into the normal state, characterized by a high surface resistance, so that the typically high Q-slope of the Nb/Cu cavities is simply due to this progressive 'micro-quench' process. Of course this phenomena is typical of the Nb/Cu cavities and cannot occur in bulk Nb cavity.

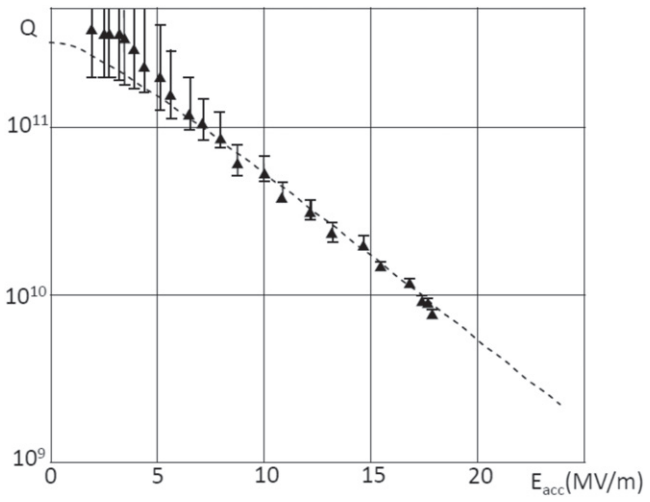

Figure 8. Q-factor versus accelerating field for a thin film Nb/Cu 1.5 GHz cavity at $T = 1.7$ K realized at CERN [6]. The triangles are the experimental points (the data are the same as those reported as triangles in figure 2 for $E_{acc} > 2$ MV m^{-1}) the dashed line represents the data fitting using the distribution function $f(R_{Nb/Cu})$ reported in figure 9.

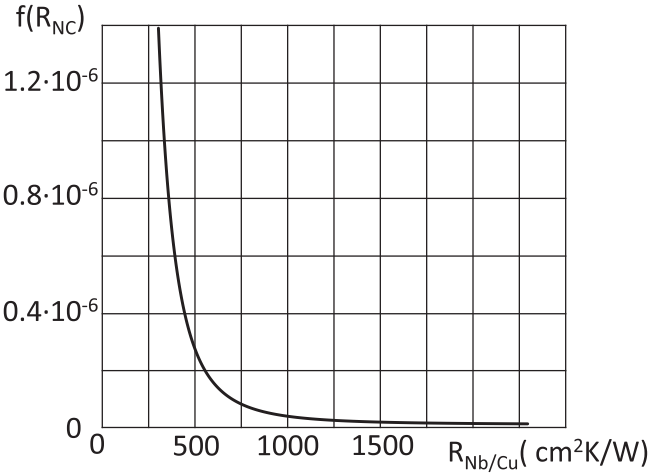

Figure 9. Distribution function $f(R_{Nb/Cu})$ obtained by inverting equation 13 using as input data the Q-E_{acc} data reported in figure 8.

It is important to remark here that the model assumes that Nb adherence problems on the high thermal conductivity Cu substrate produce local surface temperature increase, proportional to the local value of the thermal boundary resistance. This assumption is non-trivial and its validity can be more or less justified depending on the specific defect typology.

In figure 8 we present another example of a fitting procedure based on the same simple model. The data points refer to a Nb/Cu 1.3 GHz cavity measured at $T = 1.7$ K at CERN [6]. The dashed curve represents the calculation, the fitting procedure being analogous to the one reported above, starting, in this case, from the parameters reported in table 2.

In this case the precise value assumed for the Cu/He Kapitza conductance is unessential, since the thermal effects

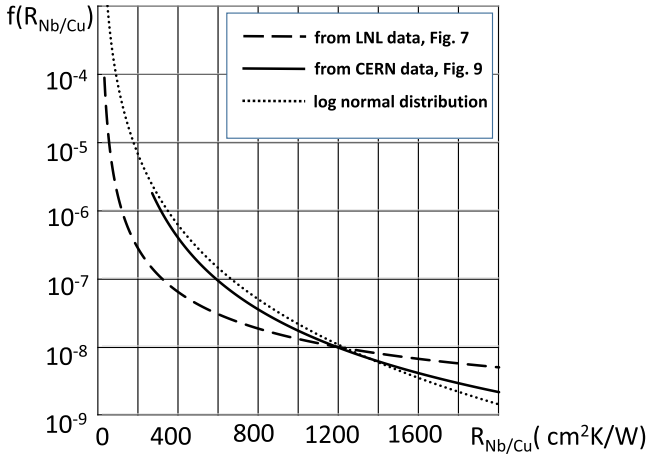

Figure 10. Comparison of the Nb/Cu thermal contact distributions assumed to fit the data reported in figures 7–9 in semi-log scale. The log-normal distribution matching the CERN data distribution is also reported.

are much less efficient for low frequency cavities and the Kapitza resistance alone in this case would determine no observable Q-slope effect in the considered field range. The global thermal quench with the assumed value for R_k would be over 200 MV m^{-1}, and this is consistent with the absence of macroscopic quench phenomena in these types of cavities up to very high fields.

The interpolating function is: $f\left(R_{Nb/Cu}\right) = 1.52 \cdot 10^6 R_{Nb/Cu}^{-\left(6.21-0.225 \ln R_{Nb/Cu}\right)}$ and is plotted in figure 9. The function is only reported for $R_{Nb/Cu}$ values above 250 cm^2 K W^{-1}: again lower $R_{Nb/Cu}$ values would affect the Q-slope above the maximum measured field ($E_{acc} = 22$ MV m^{-1}), so that the function f cannot be determined below that value.

The integral I under the represented $f(R_{Nb/Cu})$ curve in this case is extremely low ($I = 0.0003$), and it is indeed sufficient to assume that 0.03% of the Nb film in bad thermal contact with the copper substrate (or o partially detached from it) significantly contributes to the observed Q-slope. The overall percentage of the significantly detached film areas leading to values of $R_{Nb/Cu}$ well over R_K ($R_{Nb/Cu} > 2R_K > 6$ cm^2 K W^{-1}) cannot be estimated here.

Finally the distribution function for the two reported cases, plotted in linear scale in figures 7, 9 are compared in figure 10 in a semi-log scale, that better shows the distribution function behavior for high $R_{Nb/Cu}$ values. A log-normal distribution function (dotted curve in the figure) is also reported for comparison. The parameters have been adapted to match at the best the CERN data Nb/Cu thermal resistance distribution function.

In the last case for any realistic distribution function assumed for $R_{Nb/Cu} < 250$ cm^2 K W^{-1} (as an example the log-normal distribution reported in the figure) the average value of $R_{Nb/Cu}$ $\left(\overline{R_{Nb/Cu}}\right)$ calculated through equation 9, would give very small values (3–4 cm^2 K W^{-1}), which would imply a very small average temperature increase at the inner cavity surface. The value, calculated through equation (10),

would be $\overline{\Delta T} \leqslant 0.1$ K at the maximum operating field, fully justifying the already discussed negative result reported in [51].

Finally, the indication that $f(R_{Nb/Cu})$ (which represents the probability of finding a given value of the thermal resistance $R_{Nb/Cu}$) is well described by a log-normal distribution, is consistent with the hypothesis of micro-voids formed at the interface related to substrate roughness, already discussed in section 4. In fact, in the literature there is evidence that the number of micro-voids of a given diameter L grown at the film/substrate interface, can be log-normally distributed versus the ratio L/a_0, where a_0 is the lattice parameter of the film [54].

Micro-voids at the interface are mainly determined by factors such as [18, 54–58]:

i. the un-miscibility of niobium and copper as reported in [28];
ii. a limited adatom diffusivity of the niobium onto copper;
iii. an effect of self-shadowing of the growing atomic clusters;
iv. the oblique angle of deposition between cathode and substrate due to the elliptical shape of the cavity;
v. the presence of depressions or wells of the substrate that are closed by the edge deposition of two obliquely impinging fluxes, that continue to grow across the voids by interaction with the depositing atoms until a continuous bridge is formed that closes off the void.

These factors are indeed all active in Nb/Cu thin film superconducting RF cavities.

6. Discussion and conclusions

As mentioned in the introduction, solving the Q-slope problem in thin film cavities is essential for extending their use in high field accelerators. Most of the attention has been devoted in the past to improving the film quality, driven by models attributing, in different ways, the Q-slope phenomenon to the reduced film crystallinity. Other attempts were based on the idea of impurity diffusion in the film from the copper substrate. Thermal effects were also considered, but the small Nb film thickness, the high Cu thermal conductivity and theoretical estimation of the thermal boundary resistance at the Nb/Cu interface were all pointing in the direction that in thin film cavities thermal effects should be far less relevant with respect to bulk Nb cavities, excluding these effects as a possible cause of the strong Q degradation with field. This was also confirmed by a specific experimental test [51].

In this paper we have reconsidered thermal effects at the Nb/Cu interface as a possible source of the Q-slope problem. The idea was triggered by:

a. The evidence that Nb film adhesion on Cu is generally poor, due to their non-miscibility, often even causing film peel-off from the substrate.
b. A literature analysis of the thermal boundary resistance $R_{1/2}$ between two flat solid surfaces in contact [35–38], showing that in most cases, due to the non-perfect surfaces adherence $R_{1/2}$ can be indeed very high, overcoming the materials' thermal conductivity contribution up to considerable sheet thicknesses.

We have then considered that, in our case, the Nb film, due to its poor adhesion, can be partially detached from the Cu substrate in different spots of the cavity surface, giving rise to a substantially continuous distribution function $f(R_{Nb/Cu})$ of $R_{Nb/Cu}$ values over the cavity surface. We have then extended the ordinary thermal feedback models to account for these non-constant $R_{Nb/Cu}$ values over the surface. In this new frame there is a direct correspondence of the measured Q versus E_{acc} curves and $f(R_{Nb/Cu})$, so that from any measured curve, through the classical 'inverse problem' methods one can extract a corresponding distribution function of $R_{Nb/Cu}$ values that would justify the experimental data. The procedure has been applied to different sets of experimental data, two of which have been discussed in the previous section. The results appear to be very interesting:

1. In the examined cases the fraction of the cavity surface area that is relevant to determine the observed Q-slope is very small, always far less that 1%. Though a determination of the partially detached surface area (areas where the Nb/Cu thermal boundary resistance exceeds the Cu/HeII Kapitza resistance) is not possible, it appears in any case that the cavity surface fraction where the adhesion is not perfect is limited to a small percent.
2. In the examined cases the Nb/Cu thermal boundary resistance distribution functions are well approximated with a power law function, exhibiting very similar functional dependences. In the CERN data case, the distribution function can also be well approximated by a log-normal distribution. Log-normal $f(R_{Nb/Cu})$ distributions lead to Q-factor quasi-exponentially decreasing as a function of the RF injected power.

Though, in our opinion, the whole body of information and data reported in the previous sections point strongly towards the thermal mismatch at the Nb/Cu interface due to (minor) adhesion problems being the main origin of the Q-slope in thin film cavities, unfortunately there are not really any independent ways to determine the $f(R_{Nb/Cu})$ distribution independently, even using destructive methods. So we cannot furnish a full proof of our arguments. More 'tailored' measurements, including measurements at different temperatures and on sets of cavities prepared changing individual deposition parameters, will be needed to further validate the model.

Indeed, if the Nb/Cu interface thermal boundary in partially film detached areas is the source of the problem, the strategy should be addressed towards an improvement of the Nb film adhesion on the copper substrate. This can be achieved, as an example, adopting the following strategies:

1. Increasing the substrate temperature will both decrease the void volume and the mean surface roughness of the nucleating film, by increasing the spacing between void tracks.

2. Promoting the deposition kinetic energy released from the bombarding particles to the growing film could increase the film adherence. This could be done both by the application of a bias, and by an action of plasma bombardment of the growing film.
3. By growing between copper and niobium a buffer layer of a metal that is miscible to both materials for example aluminum, tin, silver or palladium.
4. Finding the right sputtering regime where the film stresses are released. Indeed by varying the noble gas pressure used for the sputtering discharge, the stress induced in the film can pass from tensile to compressive. Obviously the adhesion between copper and niobium is compromised by the film residual stress.
5. A high temperature vacuum annealing of the film after the sputtering could also play a role in the recovery of the film morphology and microstructure, especially at the interface, if the temperature is higher than 1073 K.

We are confident that experiments along these lines will finally lead to the solution of the subtle Q-slope problem in thin film accelerating cavities.

References

[1] Arnolds-Mayer G *et al* 1986 On niobium-coated copper cavities at 500 MHz *CERN Internal Report CERNIEFIRF* 86-1 (4 March)

[2] Palmieri V 2010 RF losses due to incomplete Meissner–Ochsenfeld effect: difference between bulk Nb and Nb/Cu *IV Int. Workshop on Thin Films and New Ideas for Pushing the Limits of RF Superconductivity* (*Legnaro* (*Italy*), *4–6 October 2010*) (http://slideshare.net/thinfilmsworkshop/palmieri-rf-losses-trapped-flux)

[3] Benvenuti C, Circelli N and Hauer M 1984 Niobium films for superconducting accelerating cavities *Appl. Phys. Lett.* **45** 583

[4] Palmieri V *et al* 1996 Installation in the LNL ALPI linac of the first cryostat with four niobium sputtered copper quarter wave resonators *Nucl. Instrum. Methods Phys. Res.* A **382** 112–7

[5] Venturini Delsolaro W *et al* 2013 Nb sputtered quarter wave resonators for the HIE-ISOLDE *Proc. SRF* (*Paris, September 2013*) (http://accelconf.web.cern.ch/AccelConf/SRF2013/papers/weioa03.pdf)

[6] Arbet-Engels V, Benvenuti C, Calatroni S, Darriulat P, Peck M A, Valente A-M and Van't Hof C A 2001 Superconducting niobium cavities, a case for the film technology *Nucl. Instrum. Methods Phys. Res.* A **463** 1–8

[7] Visentin B 2006 Review on Q-drop mechanisms *II Int. Workshop on Thin Films and New Ideas for Pushing the Limits of RF Superconductivity* (*Legnaro* (*Italy*), *9–12 October*) (http://lnl.infn.it/~master/slideshow/tuesday/Review%20on%20Q-drop%20mechanism_visentin.pdf)

[8] Visentin B 2003 Q-slope at high gradients: review of experiments and theories *Proc. 11th Workshop on RF Superconductivity Lübeck/Travemünder* 8–12(*September*) (http://accelconf.web.cern.ch /AccelConf/SRF2003/papers/mop19.pdf)

[9] Attanasio C, Maritato L and Vaglio R 1991 Residual surface resistance of polycrystalline superconductors *Phys. Rev.* B **43** 6128–31

[10] Hylton T L, Kapitulnik A, Beasley M R, Carini J, Drabeck L and Grüner G 1988 Weakly coupled grain model of high frequency losses in high *Tc* superconducting thin films *Appl. Phys. Lett.* **53** 1343

[11] Benvenuti C, Calatroni S, Campisi I E, Darriulat P, Peck M A, Russo R and Valente A-M 1999 Study of the surface resistance of superconducting niobium films at 1.5 GHz *Physica* C **316** 153–88

[12] Benvenuti C, Calatroni S, Campisi I E, Darriulat P, Durand C, Peck M A, Russo R and Valente A M 1997 Magnetic flux trapping in superconducting niobium *CERN-EST-97-008-SM, 8th Workshop on RF Superconductivity* v.1–v.4, Abano-Terme, Italy, 6–10 Oct pp 331–6 (http://accelconf.web.cern.ch/AccelConf/SRF97/papers/srf97b05.pdf)

[13] Benvenuti C, Calatroni S, Darriulat P and Peck M A 2001 Fluxon pinning in niobium films *Physica* C **351** 429–37 — also on CERN EST/2000-004 (SM)

[14] Bonin B and Safa H 1991 Power dissipation at high fields in granular RF superconductivity *Supercond. Sci. Technol.* **4** 257–61

[15] Kulik I O and Palmieri V 1998 Theory of Q-degradation and nonlinear effects in Nb-coated superconducting cavities *Part. Accel.* **60** 257–64

[16] Benvenuti C, Calatroni S, Campisi I E, Darriulat P, Marino M, Peck M, Russo R and Valente A M 1997 Properties of copper cavities coated with niobium using different discharge gases *CERN EST/97-04*(*SM*) *and 8th Workshop on RF Superconductivity* (*Abano-Terme, Italy, 6–10 Oct, pp 331–6*)

[17] Aberle O, Boussard D, Calatroni S, Chiaveri E, Haebel E, Hanni R, Losito R, Marque S and Tuckmantel J 1999 Technical developments on reduced-β superconducting cavities at CERN *Proc. 1999 Particle Accelerator Conf.* (*New York*) (https://cds.cern.ch/record/387156?ln=bg)

[18] Tonini D, Greggio C, Keppel G, Laviano F, Losito R, Musiani M, Torzo G and Palmieri V 2003 Morphology of niobium films sputtered at different sputtering target-substrate angle *Proc. 11th Workshop on RF Superconductivity* ed D P Lubeck (http://accelconf.web.cern.ch/AccelConf/SRF2003/papers/thp11.pdf)

[19] Lanza G *et al* 2006 New magnetron configurations for sputtered Nb onto Cu *Physica* C **441** 102
Lanza G *et al* 2005 *Proc. XII Workshop on RF Superconductivity* ed S Belomestnykh, M Liepe and H Padamsee Cornell (http://accelconf.web.cern.ch/AccelConf/SRF2005/papers/tua12.pdf)

[20] Cattarin S, Musiani M, Palmieri V and Tonini D 2006 EIS study of niobium films sputtered at different target–substrate angles *Electrochim. Acta* **51** 1745–51

[21] Bemporad E, Carassiti F, Sebastiani M, Lanza G, Palmieri V and Padamsee H Superconducting and microstructural studies on sputtered niobium thin films for accelerating cavity applications *Supercond. Sci. Technol.* **21** 125026

[22] Durand C, Weingarten W, Bosland P and Mayer J 1995 Non quadratic RF losses in niobium sputter coated accelerating structures *IEEE Trans. Appl. Supercond.* **5** 107–1110

[23] Aull S, Calatroni S, Doebert S, Junginger T, Ehiasarian A P, Knobloch J and Terenziani G 2013 RF characterization of niobium films for superconducting cavities *Proc. Int. Particle Accelerator Conf.* (*IPAC, Shanghai, China*)

[24] Isagawa S 1980 Hydrogen absorption and its effect on low-temperature electric properties of niobium *J. Appl. Phys.* **51** 4460–8
Isagawa S 1980 Influence of hydrogen on superconducting. niobium cavities *J. Appl. Phys.* **51** 6010–17

[25] Benvenuti C, Calatroni S, Hakovirta M, Neupert H, Prada M and Valente A-M 2001 CERN studies on niobium-coated 1.5 Ghz copper cavities *Proc. 10th Workshop on RF Superconductivity* (*Tsukuba, Japan*) (http://accelconf.web.cern.ch/AccelConf/srf01/papers/ma002.pdf)

[26] Benvenuti C, Calatroni S, Darriulat P, Peck M A and Valente A-M 2001 Fluxon pinning in niobium films *Physica* C **351** 429–37
[27] Kurakin G 1994 Thermal instabilities in superconducting RF cavities *4th EPAC* **III** p 2080
Haebel E 1998 Thermal feedback to explain Q drop *R&D issues in Superconduct. Cavities, TTF Meeting* TESLA vol 98-05 p 60
[28] Chakrabarti D J and Laughlin D E 1982 Cu-Nb *Bull. Alloy Phase Diagrams* **2** 455
[29] Brunner O CERN, private communication
[30] Catani L *et al* 2006 Cathodic arc grown niobium films for RF superconducting cavity applications *Physica* C **441** 130–3
Russo *et al* 2009 Niobium coating of cavities using cathodic arc *IEEE Trans. Appl. Supercond.* **19**
[31] Krishnan M 2014 Coaxial energetic deposition of thin films *Proc. VI Int. Workshop on Thin Films and New Ideas for Pushing the Limits of RF Superconductivity* (*Legnaro* (*Italy*), *6–8 October 2014*) (http://slideshare.net/thinfilmsworkshop/mahadevan-krishnan-coaxial-energetic-deposition-of-thin-films)
[32] Fujino T *et al* 1999 Promising performance of the Nb/Cu clad seamless superconducting RF cavities *Proc. 9th Workshop on RF Superconductivity* (*Santa Fè, 1–4 November*) p 372
Fujino T *et al* 2000 Development of the Nb/Cu cavities *Proc. 3rd Superconducting Linear Accelerator Meeting in Japan* (*KEK, Tsukuba, Japan, May 2000*) ed K Saito p 151
[33] Verhoeven J D and Gibson E D 1978 The monotectic reaction in Cu-Nb alloys *J. Mater. Sci.* **13** 1576–82
[34] Valente-Feliciano A M 2014 Nucleation of Nb films on cu substrates *VI Int. Workshop on Thin Films and New Ideas for Pushing the Limits of RF Superconductivity* (*Legnaro* (*Italy*), *6–8 October 2014*) (http://slideshare.net/thinfilmsworkshop/anne-marie-valente-feliciano-nucleation-of-nb-films-on-cu-substrates)
[35] Fenech H and Rohsenow W M 1962 Prediction of thermal conductance of metallic surfaces in contact *J. Heat Transfer* **85** 15
[36] Yovanovich M M and Fenech H 1966 Thermal contact conductance of nominally flat rough surfaces in a vacuum environment *Prog. Astronaut. Aeronaut.* **18** 773
[37] Cooper M G, Mikic B B and Yovanovich M M 1969 Thermal contact conductance *Int. J. Heat Mass Transfer* **12** 279
[38] Lambert M A and Fletcher L S 1997 Review of models for thermal contact conductance of metals *J. Thermophys. Heat Transfer* **11** 129
[39] Swartz E P and Pohl R O 1989 Thermal boundary resistance *Rev. Mod. Phys.* **61** 605
[40] Lyeo H K and Cahill D G 2006 Thermal conductance of interfaces between highly dissimilar materials *Phys. Rev.* B **73** 144301
[41] Oh D W, Kim S, Rogers J A, Cahill D G and Sinha S 2011 Interfacial thermal conductance of transfer-printed metal films *Adv. Mater.* **23** 5028
[42] Amrit J and Francois M X 2000 Heat flow at the niobium-superfluid helium interface: Kapitza resistance and superconducting cavities *J. Low Temp. Phys.* **119** 27
[43] Tritt T M 2004 *Thermal Conductivity: Theory, Properties, and Applications* (Berlin: Springer)
[44] Aizaz A, Grimmand T L and Wright N T 2010 Thermal design studies in superconducting rf cavities: phonon peak and Kapitza conductance *Phys. Rev. ST Accel. Beams* **13** 093503
[45] Bauer P, Solyak N, Ciovati G L, Eremeev G, Gurevich A, Lilje L and Visentin B 2006 Evidence for non-linear BCS resistance in SRF cavities *Physica* C **441** 51–6
[46] Edwards H, Cooper C A, Ge M, Gonin I V, Harms E R, Khabiboulline T N and Solyak 2009 Comparison of buffered chemical polished and electropolished 3.9 GHz cavities *TUPPO063, Proc. SRF2009* (*Berlin, Germany, September*) ed J Knobloch (http://accelconf.web.cern.ch/AccelConf/SRF2009 /papers/tuppo063.pd)
[47] Palmieri V, Rossi A A, Stark S Y and Vaglio R 2014 Evidence for thermal boundary resistance effects on superconducting radiofrequency cavity performances *Supercond. Sci. Technol.* **27** 085004
[48] Snyder N S 1970 Heat transport through helium II: Kapitza conductance *Cryogenics, APRIL* **89**
[49] Van Sciver S W 1986 *Helium Cryogenics* (New York: Plenum)
[50] Kado M M 1995 *Thermal Conductance Measurements on the LHC Helium II Heat Exchanger Pipes*, LHC Note 349, CERN-AT-95-34 CR
[51] Benvenuti C, Calatroni S, Hakovirta M, Neupert H, Prada M and Valente A-M 2001 CERN studies on niobium-coated 1.5 Ghz copper cavities *Proc. 10th Workshop on RF Supercond.* (*Tsukuba, Japan*) (http://accelconf.web.cern.ch/AccelConf/srf01/papers/ma002.pdf)
[52] Schmüser P 2003 Basic principles of RF superconductivity and superconducting cavities *Proc. CERN Accelerator School* (*Zeuthen*)
[53] Aster R C, Borchers B and Thurber C H 2012 *Parameters Estimation and Inverse Problems* 2nd edn (Amsterdam: Elsevier)
[54] Tiller W A 1991 *The Science of Crystallization: Macroscopic Phenomena and Defect Generation* (Cambridge: Cambridge University Press) ISBN-13: 978-0521388283
[55] Smith R W and Srolovitz D J 1996 Void formation during film growth: a molecular dynamics simulation study *J. Appl. Phys.* **79** 1
[56] Zexian C 2011 *Thin Film Growth Physics, Materials Science and Applications* (Sawston: Woodhead) ISBN: 978-1-84569-736-5
[57] van Kranenburg H and Lodder C 1994 Tailoring growth and local composition by oblique-incidence deposition: a review and new experimental data *Mater. Sci. Eng.* **R11** 295–354
[58] Kim S, Henderson J and Chaudhari P 1977 Computer simulation of amorphous thin films of hard spheres *Thin Solid Films* **47** 155–8